Reconfigurability Analysis of Single and Dual Wavelength Millimeter Wave Photonic Generation Techniques

Safana Alzoubi*, Mohamed Shehata†
*Technical Computer College, Damascus University. {*safana.alzoubi@gmail.com*}
†School of Electrical and Electronic Engineering, The University of Adelaide. {*mohamed.shehata@adelaide.edu.au*}

***Abstract*—Optimizing the operating conditions of a Mach-Zhender modulator (MZM) for different design requirements has drawn considerable research interests due to its key role as an electro-optic (EO) interface in hybrid access radio-over-fiber networks. In this work, we compare the modulation efficiency and the bit error rate (BER) performances of single and dual-wavelength-modulated millimeter-wave (MMW) photonic generation techniques which rely on MZMs as EO modulators. Simulation results show that although both techniques are functionally equivalent and possess the same implementation complexity, the dual wavelength modulation of a typical MZM can potentially improve the BER performance by three orders of magnitude compared to the single wavelength approach.**

***Index Terms*—Millimeter waves (MMW), modulation efficiency, optical heterodyning, photomixing, radio-over-fiber (RoF).**

I. Introduction

Among the various research efforts conducted on the fifth generation (5G)-compatible optical access networks, several techniques have been proposed to experimentally demonstrate the photonic generation of millimeter-wave (MMW) signals by heterodyning two optical frequencies, also called photo-mixing. In these techniques, the optical intensity of one or both optical carriers is modulated by a radio frequency (RF) signal via an electro-optic modulator (EOM), which is usually a Mach-Zhender modulator (MZM), resulting in single [1] or dual [2] wavelength intensity modulation (S/DW-IM) techniques, respectively. Both techniques are functionally equivalent and can be employed interchangeably to generate double-side (DSB) amplitude modulated (AM) MMW signals with or without a carrier component, depending on the MZM bias voltage.

To the best of the authors' knowledge, no study has been reported yet to investigate the major differences between both techniques in terms of the modulation efficiency and the achievable bit error rate (BER) performance. It should be highlighted that, the modulation depth of a DSB-plus-carrier (DSB+C) signal depends on the particular receiver design. For instance, a high modulation efficiency is usually desirable for energy-efficient envelope detection [3], whereas a high-power reference carrier is crucial to the performance of a self-homodyne receiver [3]. Additionally, the BER performance of each receiver type is influenced by the modulation efficiency of the received DSB+C signal. Therefore, the main objective of the comparative analysis presented in this work is to highlight the potential benefits and limitations of the SW-IM and the DW-IM-based MMW photonic generation techniques.

II. Typical Configurations of MMW Photonic Generation Techniques

Figure 1 illustrates the two considered MMW photonic generation techniques based on the photo-mixing approach, with the DW-IM configuration in Fig. 1(a) and the SW-IM configuration in Fig. 1(b). In both configurations, two optical carriers with optical powers of $P_{\mathrm{o}1}$ and $P_{\mathrm{o}2}$, and frequencies of $f_{\mathrm{o}1}$ and $f_{\mathrm{o}2}$ are emitted by two tunable laser sources (TLSs). Moreover, the MZM is biased at a DC voltage of V_B and driven by an RF signal, denoted by $v_{_{RF}}(t)$. The two optical signals are then combined and applied to a high-speed PD, which is usually a *p-i-n* photodiode, for photo-mixing.

Ideally, the PD can be modeled by a square low detector, followed by lowpass filter with a center frequency of $|f_{\mathrm{o}1} - f_{\mathrm{o}2}|$, which jointly produce the desired MMW signal. For the DW-IM, assuming small signal conditions, the DSB+C MMW electric field at the PD output is given by:

$$E_{\mathrm{MMW},1}(t) = \underbrace{\sqrt{\Re P_o}\cos^2\left(\frac{\pi V_B}{2V_\pi}\right)}_{A1}\cos\left(2\pi f_{\mathrm{MMW}}t + \Delta\varphi_n(t)\right)$$
$$+\underbrace{\frac{\pi\sqrt{\Re P_o}}{2V_\pi}\sin\left(\pi\frac{V_B}{V_\pi}\right)}_{B1} v_{_{RF}}(t)\cos\left(2\pi f_{\mathrm{MMW}}t + \Delta\varphi_n(t)\right), \quad (1)$$

where $\Re$ is the PD responsitivity, V_π is the MZM's half-wave voltage, $f_{\mathrm{MMW}} = |f_{o2} - f_{o1}|$, and $\Delta\varphi_n(t) = \varphi_{n1}(t) - \varphi_{n2}(t)$, where $\varphi_{n1}(t)$ and $\varphi_{n2}(t)$ are the random phase noises of the two TLSs. Likewise, for the SW-IM, the DSB+C MMW electric field at the PD output can be expressed as follows:

$$E_{\mathrm{MMW},2}(t) = \underbrace{\sqrt{\Re P_o}\cos\left(\frac{\pi}{2}\frac{V_B}{V_\pi}\right)}_{A2}\cos\left(2\pi f_{\mathrm{MMW}}t + \Delta\varphi_n(t)\right)$$
$$+\underbrace{\frac{\pi\sqrt{\Re P_o}}{2V_\pi}\sin\left(\frac{\pi}{2}\frac{V_B}{V_\pi}\right)}_{B2} v_{_{RF}}(t)\cos\left(2\pi f_{\mathrm{MMW}}t + \Delta\varphi_n(t)\right) \quad (2)$$

The input/output optical electric field envelope responses outlined in (1) and (2), i.e., A_1 and A_2, are plotted in Fig. 1(c). Obviously, the MZM bias voltage is a key design parameter as it controls the amounts of power contributed by the modulated DSB signal and the unmodulated carrier to the overall power of the resulting MMW signal. The modulation efficiency, defined

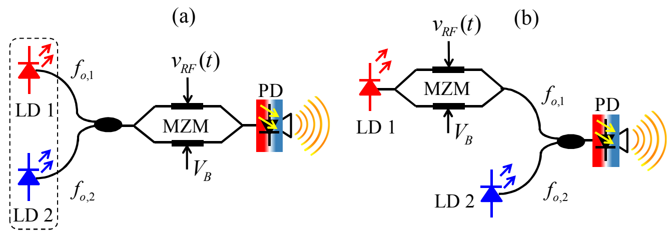

Fig. 1. Two possible topologies for millimeter wave photonic generation techniques. (a) the DW-IM topology. (b) SW-IM topology.

as the ratio of the modulating signal power to the total DSB+C signal power, is given by

$$\eta_{1,2} = \frac{B_{1,2}^2 \left\langle v_{RF}^2(t) \right\rangle}{\left(A_{1,2}^2 + B_{1,2}^2 \left\langle v_{RF}^2(t) \right\rangle\right)}, \tag{3}$$

where $\langle . \rangle$ is the time average operator, and the pairs (A_1, B_1) and (A_2, B_2) are given by (1) and (2), respectively.

III. Results and Discussion

Figure 2(a) shows the dependence of the modulation efficiency, $\eta_{1,2}$, on the amplitude of a single tone driving signal at a fixed MZM bias of $V_B = V_\pi/2$. This amplitude is allowed to increase from 0 to $V_\pi/2$ to allow the exploitation of the MZM full dynamic range by the driving sinusoid. As clear in this figure, the modulation efficiency increases monotonically when increasing the input sinusoid amplitude with the DW-IM topology is more responsive to the RF signal amplitude than its SW-IM counterpart. A maximum modulation efficiency of about 55% and 25% can be achieved by the DW-IM and the SW-IM configurations, respectively at a voltage amplitude of $V_\pi/2$. The substantial difference between η_1 and η_2 is attributed to the modulated and the unmodulated optical power components contributed by each technique to the resulting DSB MMW signal.

Furthermore, Fig. 2(b) plots the modulation efficiency achievable by each configuration when varying the MZM bias voltage, V_B, from 0 to V_π at two different values of the RF input power, namely, $P_{\mathrm{RF}} = 7$ dBm and 27 dBm. As this figure shows, at $P_{\mathrm{RF}} = 7$ dBm, the modulation efficiency of both techniques is noticeably small, i.e., less than 5%, for $V_B \leq 0.8V_\pi$. When V_B is increased beyond $0.8V_\pi$, $\eta_{1,2}$ becomes more sensitive to the variations in the MZM bias voltage and attains the close-to-unity point at $V_B = V_\pi$, which is achieved due to the suppression of the unmodulated optical carrier component as the MZM is null-biased at that point. Both configurations show very similar trends with subtle differences in the modulation efficiencies, which can be ignored in practical realizations. However, increasing P_{RF} to 27 dBm shows that, for the same MZM bias voltage, the DW-IM signal is more efficient than the SW-IM signal.

The input sinusoid is on-off keying (OOK) modulated and the MZM bias voltage is varied from 0 to V_π. The corresponding DSB modulated MMW signal is then corrupted by an additive white Gaussian noise (AWGN), demodulated and the BER is counted on a bit-by-bit basis. Figure 2(c) shows that,

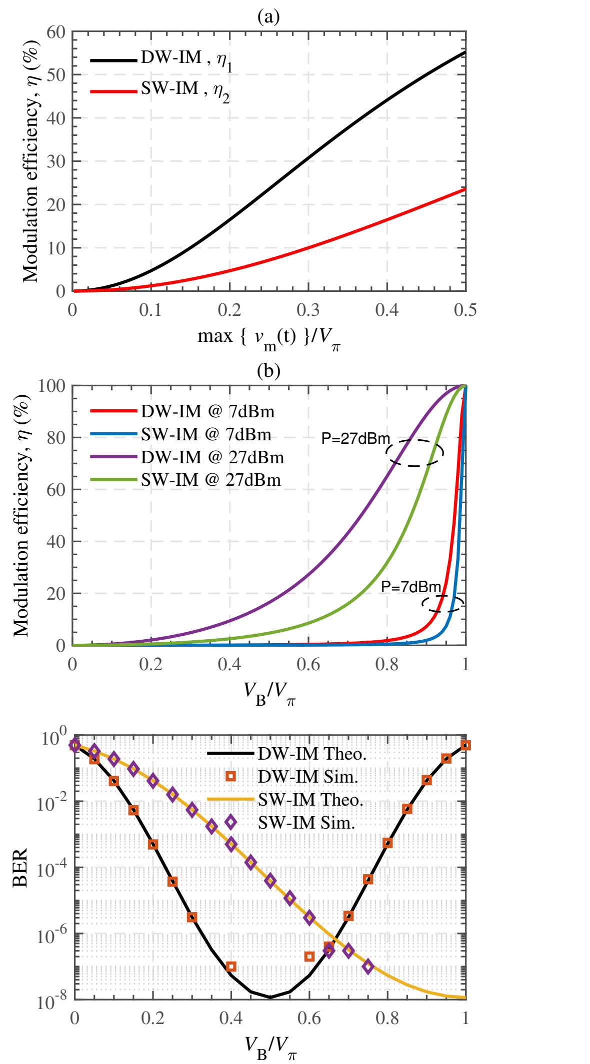

Fig. 2. Modulation efficiency for a single tone driving signal in both configurations versus (a) the modulating signal amplitude and (b) the MZM bias voltage. (c) Bit error rate performance of OOK modulation with both configurations. DW: dual wavelength. SW: single wavelength. Theo.: theoretical. Sim.: simulations.

in terms of the BER performance, the DW-IM configuration outperforms its SW-IM counterpart for $0 \leq V_B \leq 0.65V_\pi$. Moreover, this improvement is about three orders of magnitude at $V_B = 0.5V_\pi$, which is a commonly used value in the practical implementations of photonics-based MMW systems.

Our ongoing research efforts aim at confirming the obtained results experimentally by routing standard WLAN signals over a MMW radio-over-fiber system with combined optical and wireless transmission.

References

[1] C. Browning *et. al.*, "Optical heterodyne millimeter-wave analog radio-over-fiber with photonic integrated tunable lasers," in *Optical Fiber Communication Conference, Technical Digest*, paper W1I.4, (2019).

[2] P. T. Dat, *et. al.*, "High-capacity wireless backhaul network using seamless convergence of radio-over-fiber and 90-GHz millimeter-wave," in *J. Light. Technol.*, **32**, 3910-3923, (2014).

[3] J. Beas *et. al.*, "Millimeter-wave frequency radio over Fiber systems: A survey," *IEEE Commun Surv Tutor.*, **15**, 1593-1619, Fourth Quarter, (2013).